Dalton Transactions

ROYAL SOCIETY OF CHEMISTRY

PAPER

View Article Online
View Journal | View Issue

Check for updates

Cite this: *Dalton Trans.*, 2023, **52**, 16326

Not the usual suspect – an unexpected organometallic product during the synthesis of cytotoxic platinum(II) complexes†‡

Thomas Maier,[a,b] Judith Wutschitz,[a] Natalie Gajic,[a] Michaela Hejl,[a] Klaudia Cseh,[a] Sebastian Mai,[c] Michael A. Jakupec,[a,d] Mathea S. Galanski*[a] and Bernhard K. Keppler*[a,d]

Received 6th June 2023,
Accepted 29th September 2023

DOI: 10.1039/d3dt01736b

rsc.li/dalton

The reaction of (1*R*,2*R*)-(cyclohexane-1,2-diamine)dichloridoplatinum(II) with maleic acid unexpectedly resulted in the formation of an organometallic platinum(II) complex featuring a *C*,*O*-coordinating ligand. Additionally, a small series of close derivatives with increasing lipophilicity was synthesized. All complexes were fully characterized by multinuclear one- and two-dimensional (^{1}H, ^{13}C, ^{15}N, and ^{195}Pt) NMR spectroscopy, high resolution mass spectrometry, and in one case by X-ray diffraction. The lipophilicity and the impact on the DNA secondary structure as well as the cytotoxic properties in three human cancer cell lines (A549, SW480, and CH1/PA-1) were investigated. Unexpectedly, no clear-cut trend in cytotoxicity was observed with increasing lipophilicity. Also unexpectedly, the complexes showed only a low potential to inhibit cancer cell growth and no sign of interaction with DNA, in sharp contrast to the parent drug oxaliplatin, which seems to be caused by the low reactivity of the investigated compounds.

Open Access Article. Published on 06 October 2023. Downloaded on 5/28/2026 2:09:37 PM.
This article is licensed under a Creative Commons Attribution-NonCommercial 3.0 Unported Licence.

Introduction

Since Barnett Rosenberg's discovery of the antitumor activity of cisplatin,[1–4] platinum compounds have been shown to be a major force in the fight against various cancers, leading to the worldwide approval of cisplatin, carboplatin, and oxaliplatin.[5] Despite their huge success, platinum-based chemotherapy is accompanied by unfortunate drawbacks. A prominent issue is the strong side effects of these compounds, which are in some cases dose limiting. This diminishes the outcome of therapy and thus overall the rate of successful treatment. Additionally, cancers can show intrinsic or acquired resistance to platinum compounds.[6] Consequently, tuning platinum compounds towards higher activity and/or reduced side effects is still of utmost importance.

Oxaliplatin (Scheme 1) is mainly used in the case of colorectal cancer (stage II–IV), which is one of the most common causes of cancer related deaths in women and men.[7] Neurotoxicity is known to be the dose limiting toxicity. It is believed that the oxalate as leaving ligand is at least partially responsible for this toxicity. Thus, we were interested in synthesizing novel oxaliplatin derivatives, leaving the (cyclohexane-1,2-diamine)platinum(II) fragment, which is responsible for the cytotoxic properties, intact. As one of the potential dicarboxylato ligands, we have chosen maleate.

In order to synthesize the target maleato complex **2** (Scheme S1, ESI†), a standard reaction procedure was used. But to our surprise, the main product turned out to be the pair of organometallic diastereoisomers **3a**, featuring a *C*,*O*- instead of an *O*,*O*-chelating ligand as shown in Scheme 2. To the best of our knowledge, complex **3a** is mentioned only once in the literature in a patent.[8] Similar complexes with the (cyclohexane-1,2-diamine)platinum(II) moiety and a *C*,*O*-chelating ligand have been reported only scarcely. These focus mainly on ascorbato complexes,[9–19] but are not limited thereto.[20,21]

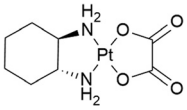

Scheme 1 Chemical structure of oxaliplatin.

[a]*University of Vienna, Faculty of Chemistry, Department of Inorganic Chemistry, Waehringer Strasse 42, 1090 Vienna, Austria. E-mail: mathea.galanski@univie.ac.at, bernhard.keppler@univie.ac.at*
[b]*University of Vienna, Doctoral School in Chemistry (DoSChem), Waehringer Strasse 42, 1090 Vienna, Austria*
[c]*University of Vienna, Faculty of Chemistry, Department of Theoretical Chemistry, Waehringer Strasse 17, 1090 Vienna, Austria*
[d]*Research Cluster "Translational Cancer Therapy Research", University of Vienna, Waehringer Strasse 42, 1090 Vienna, Austria*

† Dedicated to Prof. Wolfgang Weigand on the occasion of his 65th birthday.

‡ Electronic supplementary information (ESI) available. CCDC 2265460. For ESI and crystallographic data in CIF or other electronic format see DOI: https://doi.org/10.1039/d3dt01736b

This journal is © The Royal Society of Chemistry 2023

Open Access Article. Published on 06 October 2023. Downloaded on 5/28/2026 2:09:37 PM.
This article is licensed under a Creative Commons Attribution-NonCommercial 3.0 Unported Licence.

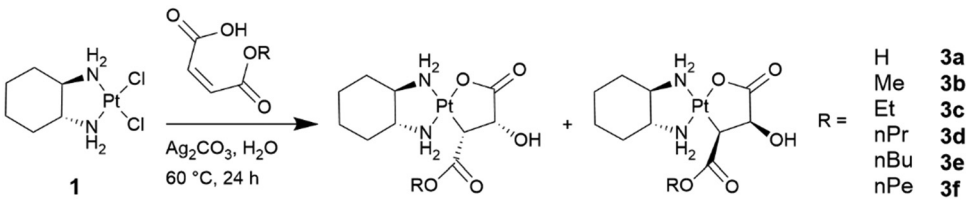

Scheme 2 Synthesis of complex **3a** and close derivatives **3b–3f**.

Furthermore, complexes with up to two coordinating nitrogen atoms and at least one coordinating carbon atom are known as well.[22–30]

With the aim of learning more about the cytotoxic properties of this type of organometallic platinum(II) complex, we additionally synthesized a small series of close derivatives with increasing lipophilicity (complexes **3b–3f**, Scheme 2). The target complexes were fully characterized by one- and two-dimensional multinuclear (^{1}H, ^{13}C, ^{15}N, ^{195}Pt) NMR spectroscopy and high-resolution mass spectrometry and were investigated with respect to their cytotoxic properties in three human cancer cell lines and for their impact on the DNA secondary structure in a cell-free assay.

Results and discussion

Synthesis and characterization

Dichloridoplatinum(II) complex **1** was suspended in water and mixed with maleic acid in the presence of Ag_2CO_3 (Scheme 2). The silver salt thereby has a double function. (i) It reacts efficiently with chloride ions of **1**, producing the soluble diaquaplatinum(II) complex and insoluble silver chloride. (ii) The reaction of maleic acid with the activated platinum species is accelerated, since acidic protons of the chelating ligand react with carbonate, releasing CO_2 from the solution. As delineated above, the organometallic species **3a** was isolated and not the expected dicarboxylato species **2**. X-ray diffraction quality single crystals of **3a** were obtained directly from the reaction solution (Fig. 1).

For brevity, the following discussion references only the values of one diastereoisomer of **3a** (Fig. 1). The same correlations are found for the second diastereoisomer, albeit with small deviations in absolute numbers. The platinum(II) ion has a square-planar PtN_2CO coordination geometry and is chelated by two bidentate ligands: (1*R*,2*R*)-*trans*-(cyclohexane-1,2-diamine) and 2-hydroxybutanedioic acid. The diamine ligand acts as a neutral ligand coordinating to the platinum center *via* nitrogen atoms N1 and N2. The second ligand is doubly negatively charged and bound to platinum(II) through oxygen atom O17 and carbon atom C9. The cyclohexane ring adopts a chair conformation and both amine groups are in the equatorial position. A distorted envelope conformation is found in both five-membered chelate rings. The torsion angle serves as a measure of deviation from the planarity of the chelate ring, which was found to be −56(1)° ($\Theta_{N1-C1-C2-N2}$), and −30(2)° ($\Theta_{O17-C8-C7-C9}$), respectively. The two diastereoisomers differ in the orientation of the substituents of the *C*,*O*-chelating ligand (compare Scheme 2). Either the carboxyl group, the hydroxyl group and the neighboring N–CH hydrogen atom point in one direction relative to the PtN_2CO coordination plane, or the COOH and OH both point to one side and the respective N–CH hydrogen atom to the opposite side.

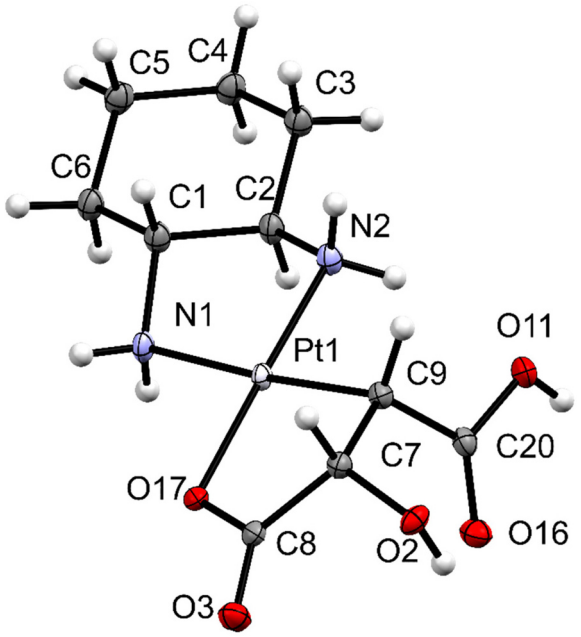

Fig. 1 ORTEP view of complex **3a**. One of the two diastereoisomers in the asymmetric unit of **3a** is drawn with 50% displacement ellipsoids. Solvent molecules are omitted for clarity. Selected bond lengths (of the shown diastereoisomer) [Å]: Pt1–N2: 2.032(12), Pt1–N1: 2.118(13), Pt1–O17: 2.053(10), Pt1–C9: 2.054(14), and C9–C7: 1.512(14) and selected angles [°]: N2–Pt1–N1: 82.1(5), N1–Pt1–O17: 98.4(4), O17–Pt1–C9: 85.5(4), and C9–Pt1–N2: 94.1(5).

The hydroxyl and the carboxyl substituents at C7 and C9 are placed in the *cis* configuration. The C7–C9 bond length of 1.512(14) Å is in the typical range of a C–C single bond; the vicinal protons H(C7) and H(C9) feature a torsion angle $\Theta_{H-C7-C9-H}$ of 32°.

The Pt–C bond [2.054(14) Å] is shorter than the corresponding bond of an ascorbatoplatinum(II) complex, Pt(en)(C^2, O^5-Asc) [2.126(4) Å].[19] The Pt–N bond length is dependent on the coordinated atom in the *trans* position. Due to the higher *trans* effect of the bound σ-carbon atom compared to co-

Open Access Article. Published on 06 October 2023. Downloaded on 5/28/2026 2:09:37 PM.
This article is licensed under a Creative Commons Attribution-NonCommercial 3.0 Unported Licence.

ordinated oxygen, the Pt–N bond *trans* to the carbon atom [Pt1–N1, 2.118(13) Å] is longer than that *trans* to oxygen [Pt1–N2, 2.032(12) Å]. This observation is in accordance with those values reported for Pt(en)(C^2,O^5-Asc) [2.083(3) *versus* 2.052(3) Å].[19]

Synthesis of complex **3a** was reproducible and has subsequently been optimized. Recrystallization from water by treatment with activated charcoal improved the appearance of the product. However, recrystallization was omitted for further batches and only activated charcoal was added approximately 5 min before filtering off the precipitated AgCl. This led to a drastic increase in yield, from 20% to 59%, while no significant decrease in purity was observed.

The reaction of dichlorido(*trans*-1*R*,2*R*-cyclohexane-1,2-diamine)platinum(II), **1**, with maleic acid results in the formation of two diastereoisomers with either 10*S*,11*R*- or 10*R*,11*S*-configuration in the C^{11},*O*-chelating ligand (the NMR numbering scheme for all synthesized compounds is shown in Fig. S1 in the ESI†). The isomers could not be separated by preparative HPLC. Consequently, a doubled set of NMR signals is found in ^{1}H, ^{13}C, ^{15}N, and ^{195}Pt NMR spectra, making complete peak assignment more complicated. Most indicative of the PtN_2CO coordination sphere, besides the absence of the double bond, in diastereoisomers of **3a** are the ^{195}Pt chemical shifts at −1280.2 and −1282.4 ppm, respectively. In contrast, a ^{195}Pt resonance at around −400 ppm was expected for complex **2** exhibiting a PtN_2O_2 coordination. These values and differences in ^{195}Pt chemical shifts are well comparable with those found in the literature for ascorbatoplatinum(II) complexes in the Pt(en)(C^2,O^5-Asc) or Pt(en)(O^2,O^3-Asc) coordination mode at −1060 and −96 ppm, respectively.[19]

Finally, peak and signal assignments to both diastereoisomers were performed on the basis of two-dimensional homonuclear and heteronuclear NMR spectroscopy. Most useful was recording the [^{1}H,^{195}Pt] HSQC spectrum (Fig. 2). As a result, specific protons of the isolated spin systems of the cyclohexanediamine (NH protons), as well as those of the *C*,*O*-chelating ligand (protons H11), show shift correlation signals with the ^{195}Pt atom of the respective diastereoisomer. From these anchor points, diastereoisomer A and B were defined and peaks were further assigned with the help of [^{1}H,^{1}H] COSY, [^{1}H,^{13}C] HSQC, [^{1}H,^{13}C] HMBC, and [^{1}H,^{15}N] HSQC NMR spectroscopy.

However, the complete assignment of every single signal was limited in the case of overlapping signals, especially that of protons in the cyclohexane ring or of ^{13}C resonances, featuring small differences in their chemical shifts due to the diastereoisomeric nature of **3a** (Fig. 3). Additionally, complex **3a** was further characterized by high resolution mass spectrometry and elemental analysis.

Complex **3a** has good water solubility. Since the cytotoxic properties of compounds are in part dependent on their lipophilicity, close analogues of **3a** have additionally been synthesized (Scheme 2). For that purpose, first the respective mono esters of maleic acid were prepared by adjusting a procedure from the literature[31] from maleic anhydride and the respective alcohol. Target complexes **3b–3f** were synthesized and purified *via* preparative HPLC in an isocratic fashion using acetonitrile and MilliQ water with 0.1% formic acid as the additive. Separation of the diastereoisomers was not possible with the utilized chromatography setup. Compounds **3b–3f** were fully characterized by multinuclear NMR spectroscopy, high resolution mass spectrometry and elemental analysis. Again, in accordance with complex **3a**, novel platinum(II) compounds showed for nearly every single atom a double set of signals in NMR spectra due to the presence of two diastereoisomers. For example, two ^{195}Pt chemical shifts for complexes **3b–3f** were found in the region between −1273 and −1285 ppm, which were separated by 2–9 ppm. As expected, these signals are well comparable with ^{195}Pt resonances of −1280.2 and −1282.8 ppm in the case of compound **3a**.

Cytotoxicity

Cytotoxicity was investigated in three human cancer cell lines differing in their general chemosensitivity: the multidrug-resistant non-small cell lung cancer cell line A549, the colon

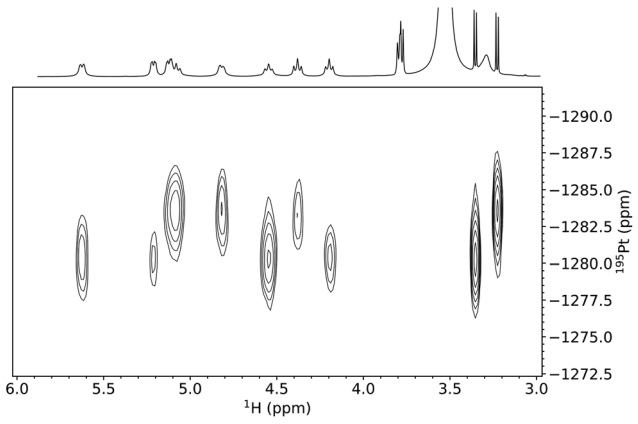

Fig. 2 [^{1}H,^{195}Pt] HSQC spectrum of **3a** showing shift correlation signals between ^{195}Pt resonances of both diastereoisomers and NH protons (4.1–5.8 ppm) as well as protons H11 at 3.23 and 3.35 ppm.

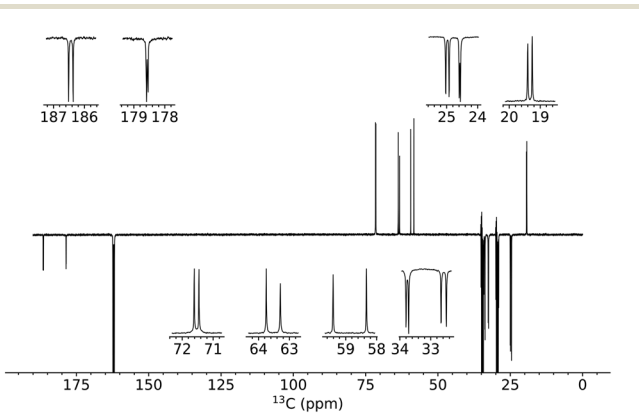

Fig. 3 ^{13}C NMR spectrum of complex **3a**. The zoomed double peaks show the diastereomeric nature of the product.

This journal is © The Royal Society of Chemistry 2023

Open Access Article. Published on 06 October 2023. Downloaded on 5/28/2026 2:09:37 PM. This article is licensed under a Creative Commons Attribution-NonCommercial 3.0 Unported Licence.

cancer cell line SW480 with mostly intermediate sensitivity, and the quite broadly sensitive ovarian teratocarcinoma cell line CH1/PA-1. The IC_{50} values were interpolated from the concentration–effect curves (Fig. S2, ESI†) and are listed in Table 1. Overall, complexes **3a–3f** have low cytotoxic potencies, which was unexpected for organometallic platinum(II) complexes at first sight. This observation is even more unexpected taking into consideration that **3a–3f**, upon release of the chelating ligands, are expected to form the same bisadducts with DNA as oxaliplatin. Consequently, the high IC_{50} values most probably reflect the low reactivity of the compounds. One further contribution to the low cytotoxicity of compound **3a** could be its deprotonation under physiological conditions. The attack of the resulting negatively charged species on DNA would be hampered, since DNA is also negatively charged. This assumption would only hold true if complex **3a** arrives intact at the DNA without the ligand exchange reaction.

With regard to cell line dependency, the IC_{50} values of **3a–3f** follow the expected trend for oxaliplatin derivatives: A549 > SW480 > CH1/PA-1, but they are by factors of ~100 to >500 less potent than the parent drug oxaliplatin. This observation is difficult to explain and warrants further investigation. The literature data for reasonable comparison are scarce: a shikimate based DACH Pt(II) complex bearing a *C*,*O*-coordination motif has been reported to yield an IC_{50} value of 3.2 μM (after 72 h of exposure for L1210 murine leukemia cells), which is 80 times higher than that of [Pt(DACH)SO_4] (with oxaliplatin not included in this study); nevertheless, *in vivo* activity has been claimed for this compound.[20] An only remotely related dinuclear Pt(II) complex containing a bridging *C*,*N*-chelating benzohydroxamate ligand has been found to be five times less potent after 72 h of exposure of A2780 ovarian cancer cells than the mononuclear [Pt(DACH)Cl_2] (with oxaliplatin not included either).[21] Even if seemingly more pronounced, the reduced cytotoxicity of complexes described here is in line with these reports.

DNA-interaction assay

A dsDNA plasmid assay was performed to check whether DNA could be the main target of the tested compounds like for the conventional platinum drugs.[33] Additionally, this assay is useful in judging the reactivity of compounds towards DNA. The native plasmid is mainly present in the negatively supercoiled (sc) form, but upon interaction with compounds, it may, depending on the kind of interaction, adopt an open circular (oc), linear or cross-linked form. As has been shown recently, cisplatin interacts with plasmid DNA relatively fast.[33] Total untwisting of the supercoiled form to the open circular form was already found after 30 min. In the case of oxaliplatin, featuring a bidentate oxalate ligand, pronounced interaction with dsDNA plasmid starts after 4 hours. However, complexes **3a** and **3d** showed no ability to untwist or break the supercoiled form towards the open circular or linear forms within 6 hours of incubation. Therefore, compounds **3a** and **3d** do not show any signs of DNA cross-linking or strand breaking under these conditions (Fig. S3, ESI†).

Table 1 IC_{50} values and lipophilicity of the synthesized complexes. IC_{50} values are means ± standard deviations from at least three independent MTT assays (96 h exposure)

	A549	SW480	CH1/PA-1	$\log k_w$
3a [a]	>200	91 ± 17	42 ± 6	0.17
3a	>200	32 ± 5	20 ± 4	
3b	>200	166 ± 9	102 ± 13	0.64
3c	>200	147 ± 4	105 ± 22	1.15
3d	164 ± 25	42 ± 2	25 ± 9	1.20
3e	>200	96 ± 11	47 ± 8	2.01
3f	>200	136 ± 34	37 ± 4	2.38
Oxaliplatin	0.98 ± 0.21[b]	0.29 ± 0.05[b]	0.18 ± 0.01[b]	0.24

[a] Crystals dissolved in DMSO and then diluted in the medium; all other samples were prepared from lyophilized compounds and directly dissolved in the medium. [b] As previously reported in ref. 32.

Lipophilicity

Due to the low cytotoxicity and the absence of interaction with isolated DNA, we investigated the lipophilicity of the synthesized complexes in comparison with oxaliplatin in order to shed more light on their modes of action. Lipophilicity is a crucial parameter in drug discovery, since it has a great influence on the diffusion of drugs through cell membranes, or it affects how efficiently drugs are distributed in body tissue rather than plasma. The lipophilic properties of complexes **3a–3f** in comparison with oxaliplatin were determined *via* an HPLC-based method as reported previously.[34] The change in the retention time on a C18 HPLC column with varying contents of the organic modifier was used to determine the $\log k_w$ values. As expected, the lipophilicity increases from **3a** to **3f** (Table 1), while the lipophilic properties of complex **3a** are well comparable with those of oxaliplatin.

Unexpectedly, there was no clear-cut dependency between the lipophilicity and cytotoxicity of complexes **3a** to **3f**. Usually, the cellular accumulation of compounds is facilitated by increasing lipophilicity, resulting in decreasing IC_{50} values, within homologous series of complexes. This deviation might be explained by two opposing effects: increasing lipophilicity on the one hand, but a concurrently increasing steric demand affecting cytotoxicity on the other.

Reactivity towards 5′-GMP

The cytotoxicity of **3a–3f** is remarkably low and interaction with DNA was not observed for compounds **3a** and **3d**. In contrast, the lipophilic properties of complexes are comparable with (**3a**) or better (**3b–3f**) than those of clinically established oxaliplatin, suggesting improved antiproliferative activity. Accordingly, it seems to be obvious that reactivity plays a crucial role in their mode of action. Since guanine in cellular DNA is known to be the most important target of platinum based drugs,[35] the reactivity of **3a** in comparison with oxaliplatin towards 5′-GMP as a model nucleotide was investigated. Thus, oxaliplatin and complex **3a**, respectively, were incubated

Open Access Article. Published on 06 October 2023. Downloaded on 5/28/2026 2:09:37 PM.
This article is licensed under a Creative Commons Attribution-NonCommercial 3.0 Unported Licence.

with a 10-fold excess of 5′-GMP. The corresponding HPLC traces are depicted in Fig. S4–S6 of the ESI.†

First, the stability of 5′-GMP, oxaliplatin and complex **3a** was investigated in PBS buffered solution at pH 7.4 over 194 h. 5′-GMP is stable in PBS under the chosen conditions (Fig. S6, ESI†). In contrast, oxaliplatin is not fully stable in PBS. This can be seen in the decrease of the oxaliplatin peak at rt = 0.8 min over time accompanied by an increase in the peak at rt = 0.35 min. Furthermore, deposition of yellow crystals in the HPLC vial was observed. Presumably, oxaliplatin reacts with Cl^- ions from the buffered solution (PBS), yielding complex **1**, which is sparsely soluble in water. Complex **3a** is fairly stable in PBS over the course of the assay. A very slow increase in the peak at rt = 0.45 accompanied by a very slow decrease in the compound peak at rt = 0.9 min shows only minor decomposition (Fig. S5, ESI†).

In the presence of 5′-GMP, the oxaliplatin containing sample shows a fast reaction of oxaliplatin with the nucleotide (Fig. S4, ESI†). In contrast, in comparison with oxaliplatin, complex **3a** reacts very slowly with 5′-GMP (compare Fig. S4 and S5 of the ESI†).

Reactivity assessment *via* DFT calculations

In order to exclude possible differences in reactivity due to protonation or deprotonation of the carboxylic acid moiety of complex **3a**, DFT calculations were performed. The starting point for these optimizations was the geometry provided by crystal structure measurements. Comparison of the optimized geometries with the data obtained from X-ray crystallography shows only minor differences (Fig. S28 of the ESI†).

Since the Pt–C bond length of the protonated complex **3a** is well comparable with that of the deprotonated complex (2.061 *vs.* 2.044 Å for molecule A and 2.019 *vs.* 2.062 Å for molecule B), the thermodynamic stability is not significantly different (Fig. S29 of the ESI†).

Conclusions

Six platinum(II) complexes related to oxaliplatin, but with *C*,*O*-chelating maleic acid derived ligands, were prepared, five of them, to the best of our knowledge, for the first time. Overall, the cytotoxic potency of this class of organometallic compounds was unexpectedly low, and in contrast to oxaliplatin (as shown previously), no evidence for cross-linking was obtained upon cell-free interaction with a dsDNA plasmid. In addition, the reaction with the model nucleotide 5′-GMP was also very slow compared to oxaliplatin. It can be concluded that such types of organometallic platinum complexes feature very low reactivity. Remarkably, cytotoxic activity could not be steadily improved by increasing the lipophilicity. Additionally, it seems that the steric bulk in the *C*,*O*-chelating ligand has an opposing effect. All these observations warrant further synthesis of close analogues and comparative studies of selected representatives of this remarkable class of platinum-based complexes.

Methods and experimental

General

All solvents and chemicals were obtained from commercial suppliers and used as received. $K_2[PtCl_4]$ was bought from Johnson Matthey (Switzerland). Water was purified with a MilliQ system (Milli-Q, 18.2 MΩ cm^{-1}, Milli-Q Advantage A10, Darmstadt, German). Although all products seem to be bench stable, reactions involving platinum complexes were conducted under protection from light. Unless stated otherwise, all reactions were performed in 20 mL scintillation vials and stirred with PTFE coated stirring bars. Vials were heated with an aluminum heating block.

Analytical HPLC measurements were performed on a Thermo Fisher HPLC with a DAD detector and an Acquity UPLC BEH C18 1.7 μm column (3.0 × 50 mm) or an Agilent HPLC-MS with the same column and a dual wavelength detector. For all analyses, the 220 nm channel was used; additionally, MS data from HPLC-MS were used for the identification of product peaks. Lipophilicity measurements were conducted on the same Thermo Fisher device using the same Acquity UPLC BEH C18 1.7 μm column (3.0 × 50 mm). Data collection for analytical HPLC was done using Chromeleon 7.2 SR5 from Thermo Scientific. Preparative HPLC was performed on an Agilent preparative HPLC system with an Xbridge Prep C18 10 μm column (19 × 250 mm). Procedures for purification *via* preparative HPLC were developed *via* optimizing isocratic methods on the analytical setup.

NMR experiments were performed with a Bruker Avance NEO 500 MHz spectrometer at 500.32 (^{1}H), 125.81 (^{13}C), 107.55 (^{195}Pt) and 50.70 (^{15}N) MHz in DMF-d_7, D_2O or $CDCl_3$ at 298 K. The (residual) solvent resonances were used as the internal reference for ^{1}H (DMF-d_7, 2.93 ppm, low-field methyl signal;[34] $CDCl_3$, 7.26 ppm (ref. 36)) and ^{13}C (DMF-d_7, 34.6 ppm, low-field methyl signal;[34] $CDCl_3$ 77.16 ppm (ref. 36)) chemical shifts. ^{195}Pt and ^{15}N signals were referenced relative to external $K_2[PtCl_4]$[34] or NH_4Cl, respectively. The NMR numbering scheme for all synthesized compounds is shown in Fig. S1 in the ESI.†

Elemental analyses were performed with a PerkinElmer 2400 CHN Elemental Analyzer or an Eurovector EA 3000 CHNS-O elemental analyzer at the Microanalytical Laboratory of the University of Vienna.

ESI-MS was performed with a Bruker maXis UHR-TOF spectrometer in the positive and negative mode using ACN/MeOH 1/1 with 1% water as the solvent (ACN = acetonitrile).

Single crystal X-ray diffraction data were collected with a Stadivari diffractometer (STOE & Cie GmbH, Germany) equipped with an EIGER2 R500 detector (Dectris Ltd, Switzerland). Data were processed and scaled with the STOE software suite X-Area (STOE & Cie GmbH). Structures were solved using SHELXT[37] and refined with SHELXL[38] or Olex2.[39] Model building was carried out using Olex2 or ShelXle.[40] Structures were validated using CHECKCIF (**https://checkcif.iucr.org/**). Please see the respective CIF files for exact versions and more details. An overview of the sample and crystal data,

This journal is © The Royal Society of Chemistry 2023

Open Access Article. Published on 06 October 2023. Downloaded on 5/28/2026 2:09:37 PM. This article is licensed under a Creative Commons Attribution-NonCommercial 3.0 Unported Licence.

data collection and structure refinement, as well as an overview of bond lengths and angles for complex **3a** can be found in Tables S1–S3 in the ESI.† The ORTEP view of complex **3a** drawn with 50% displacement ellipsoids is shown in Fig. S30 in the ESI.†

Determination of lipophilicity *via* RP-HPLC

Analyte solutions with a concentration of 0.5 mM were prepared in an ACN/MilliQ water mixture consisting of 90% (v/v) MilliQ water and 10% (v/v) ACN. This solvent was acidified with 0.1% (v/v) formic acid. The retention time was determined for three different, isocratic eluent mixtures on a Thermo Fisher HPLC system. Evaluation of the 220 nm channel *via* an established method[34,41] gave the listed $\log k_w$ values.

Cytotoxicity test

Adherent CH1/PA-1 ovarian teratocarcinoma cells (a donation from Lloyd R. Kelland, CRC Centre for Cancer Therapeutics, Institute of Cancer Research, Sutton, UK), as well as SW480 colon and A549 lung adenocarcinoma cells (both kindly provided by the Institute of Cancer Research, Department of Medicine I, Medical University of Vienna, Austria) were grown in minimal essential medium supplemented with 10% v/v heat-inactivated fetal bovine serum (Biowest, Nuaillé, France), 4 mM L-glutamine, 1 mM sodium pyruvate and 1% v/v non-essential amino acids (from a ready-to-use solution) at 37 °C under 5% CO_2. All culture media, supplements and reagents were purchased from Sigma Aldrich (St Louis, MO, USA) and all plasticware from Starlab (Hamburg, Germany), unless stated otherwise.

Cytotoxicity of the compounds was determined by using the colorimetric MTT assay (MTT = 3-(4,5-dimethyl-2-thiazolyl)-2,5-diphenyl-2*H*-tetrazolium bromide). CH1/PA-1, SW480 and A549 cells were harvested by trypsinization and seeded in 96-well flat-bottom microculture plates at densities of 1×10^3, 2×10^3 and 3×10^3 cells (100 μL per well), respectively. Cells were allowed to settle for 24 h to resume exponential adherent growth. Test compounds were dissolved and serially diluted in a supplemented medium and then added in aliquots of 100 μL to each well. After continuous exposure for 96 h, the drug-containing medium was replaced with 100 μL of an RPMI 1640 medium/MTT mixture [6 parts of the RPMI 1640 medium (supplemented with 10% heat-inactivated fetal bovine serum and 2 mM L-glutamine) and 1 part of MTT in phosphate-buffered saline (5 mg mL^{-1})] per well. After incubation for 4 h, the mixtures were removed, and the formazan crystals formed by viable cells were dissolved in 150 μL of DMSO per well. Optical densities at 550 nm were measured with a microplate reader (ELx808, Bio-Tek, Winooski, VT, USA), using a reference wavelength of 690 nm to correct for unspecific absorption. 50% inhibitory concentrations (IC_{50}) were interpolated from concentration–effect curves based on quantities of viable cells relative to untreated controls. Data are means from at least three independent experiments, each with triplicates per concentration.

DNA-interaction assay

Stock solutions of **3a** and **3d** (5 mM) were prepared in MilliQ water and respective volumes were added to reaction solutions to obtain 50 μM of the test compounds. 0.1 μg μL^{-1} pUC19 dsDNA (2686 bp) plasmid (New England BioLabs) was exposed to the compounds for different time intervals (15 min to 6 h) at 37 °C under continuous shaking. 20 μL of the samples was added to 4 μl of 6x DNA loading dye (ThermoFisher Scientific) and loaded onto a 1% agarose gel in 1× TBE buffer. Electrophoresis was performed at 60 V for 5 min, followed by 120 V for 90 min. Ethidium bromide (Serva) staining was carried out in 1× TBE (0.75 μg ml^{-1}) for 20 min. Images were taken using the GelDoc-It Imaging System Fusion Fx7 (Vilber Lourmat, Germany).

Reaction towards 5′-GMP

The following three stock solutions were prepared in phosphate buffered saline (PBS; commercially available powder yielding 0.2 g L^{-1} KCl, 0.2 g L^{-1} KH_2PO_4, 8.0 g L^{-1} NaCl, and 2.26 g L^{-1} Na_2HPO_4 anhydrous) at a pH value of 7.4: 0.005 mM oxaliplatin (stock A), 0.005 mM complex **3a** (stock B) and 0.05 mM 5′-guanosine monophosphate disodium salt (5′-GMP) (stock C).

From these solutions, five samples (1 mL each) were prepared: stock A diluted 1 : 1 with PBS, stock B diluted 1 : 1 with PBS, stock C diluted 1 : 1 with PBS, stock A combined 1 : 1 with stock C and stock B combined 1 : 1 with stock C.

After thorough mixing and subsequent filtration through a Minisart® RC4 Syringe filter, the samples were measured immediately on a Thermo Fisher HPLC and kept at 36.9 °C in the autosampler for 26 h. Subsequently, they were transferred to an aluminium heating block at 37 °C. During the first 7 hours, each sample was measured approximately every 48 min. Further measurements were performed at 26 h, 100 h and 194 h. The obtained chromatograms were compared in a qualitative fashion. The peaks were identified *via* their respective *m*/*z* values, measured *via* injecting the same samples into an Agilent HPLC-MS under the same chromatographic conditions.

DFT calculations

Computational approach. The geometry for diastereoisomer B was taken from the cif file, whereas the geometry of diastereoisomer A was obtained by changing appropriate dihedrals. These diastereoisomers as well as their analogues, which were obtained by removing the proton from the carboxyl group, served as starting geometries. For these four geometries, optimization was performed and the final geometries were obtained. Frequency calculations confirmed that minima were obtained in all cases.

Computational details. The optimizations and frequency calculations were performed using ORCA 5.0.4.[42] The electronic structure level of theory was PBE0/def2-TZVP,[43,44] using the def2-ECP effective core potential[43] for Pt. The D3BJ dispersion correction[45] and implicit solvation (C-PCM[46] for water) were

Open Access Article. Published on 06 October 2023. Downloaded on 5/28/2026 2:09:37 PM. This article is licensed under a Creative Commons Attribution-NonCommercial 3.0 Unported Licence.

employed. The RIJCOSX approximation[47] with the SARC/J Coulomb fitting basis set[48,49] was used to accelerate the calculation.

Syntheses

Synthesis of complex 1. K_2PtCl_4 (5 g, 12.05 mmol) was added to a solution of (1*R*,2*R*)-cyclohexane-1,2-diamine (1.38 g, 12.05 mmol) in 100 mL of MilliQ water in a 250 mL round bottom flask and stirred overnight. The yellow precipitate was filtered off, washed with ice cold water, EtOH and Et_2O and dried *in vacuo*.

Yield: 4.09 g (89%). EA: ($C_6H_{14}N_2Cl_2Pt$): C 18.95% H 3.71% N 7.37%; found: C 18.83% H 3.68% N 7.24%. ^{1}H NMR (DMF-d_7, 500.32 MHz): δ = 1.16 (m, 2H, H4/H5 ax), 1.49 (m, 2H, H3/H6 ax), 1.56 (m, 2H, H4/H5 eq.), 2.10 (m, 2H, H3/H6 eq.), 2.60 (m, 2H, H1/H2), 5.06 (m, 2H, H7/H8 ax), 5.62 (m, 2H, H7/H8 eq.) ppm. ^{13}C NMR (DMF-d_7, 125.81 MHz): δ = 24.46 (C4/C5), 31.96 (C3/C6), 63.32 (C1/C2) ppm. ^{15}N NMR (DMF-d_7, 50.70 MHz): δ = −20.1 ppm. ^{195}Pt NMR (DMF-d_7, 107.57 MHz): δ = −654.5 ppm. HR-MS: m/z = 403.0048 g mol^{-1} *vs.* calc. 403.0055 g mol^{-1} [M + Na$^+$].

General procedure (1) for the synthesis of maleic acid mono esters.[31] Maleic anhydride (10 g, 0.1 mol) and Na_2CO_3 (5.51 g, 0.05 mol) were suspended in the corresponding alcohol (50 mL) in a round bottom flask and stirred at room temperature. After 2 hours, the alcohol was evaporated *in vacuo*. The crude product was dissolved in 20 mL of MilliQ water and acidified with conc. HCl. The solution was extracted with EtOAc. The combined organic phases were washed with brine, dried over $MgSO_4$, evaporated and dried *in vacuo*. No further purification was performed.

Synthesis of (*Z*)-4-oxo-4-propoxybut-2-enoic acid. Synthesized according to general procedure (**1**) from 1-propanol.

Yield: 14.05 g (88%). ^{1}H NMR ($CDCl_3$, 500.32 MHz): δ = 0.97 (t, J(^{1}H,^{1}H) = 7.4 Hz, 3H, H7), 1.74 (sex, J(^{1}H,^{1}H) = 7.1 Hz, 2H, H6), 4.23 (t, J(^{1}H,^{1}H) = 6.6 Hz, 2H, H5), 6.37 (d, J(^{1}H,^{1}H) = 12.8 Hz, 1H, H3), 6.43 (d, J(^{1}H,^{1}H) = 12.6 Hz, 1H, H2), 10.73 (s(b), 1H, H1) ppm. ^{13}C NMR ($CDCl_3$, 125.81 MHz): δ = 10.34 (C7), 21.73 (C6), 68.63 (C5), 129.85 (C3), 135.64 (C2), 165.40 (C4), 167.75 (C1) ppm. HR-MS: m/z = 181.0471 g mol^{-1} *vs.* calc. 181.0471 g mol^{-1} [M + Na$^+$].

Synthesis of (*Z*)-4-butoxy-4-oxobut-2-enoic acid. Synthesized according to general procedure (**1**) from 1-butanol.

Yield: 14.23 g (83%). ^{1}H NMR ($CDCl_3$, 500.32 MHz): δ = 0.94 (t, J(^{1}H,^{1}H) = 7.3 Hz, 3H, H8), 1.40 (sex, J(^{1}H,^{1}H) = 7.5 Hz, 2H, H7), 1.68 (p, J(^{1}H,^{1}H) = 7.1 Hz, 2H, H6), 4.26 (t, J(^{1}H,^{1}H) = 6.6 Hz, 2H, H5), 6.36 (d, J(^{1}H,^{1}H) = 12.8 Hz, 1 h, H3), 6.42 (d, J(^{1}H,^{1}H) = 13.0 Hz, 1H, H2), 11.17 (s(b), 1H, H1) ppm. ^{13}C NMR ($CDCl_3$, 125.81 MHz): δ = 13.67 (C8), 19.07 (C7), 30.29 (C6), 66.91 (C5), 129.93 (C3), 135.40 (C2), 165.54 (C4), 167.68 (C1) ppm. HR-MS: m/z = 173.0808 g mol^{-1} *vs.* calc. 173.0808 g mol^{-1} [M + H$^+$].

Synthesis of (*Z*)-4-oxo-4-(pentyloxy)but-2-enoic acid. Synthesized according to general procedure (**1**) from 1-pentanol.

Yield: 16.42 g (88%). ^{1}H NMR ($CDCl_3$, 500.32 MHz): δ = 0.90 (m, 3H, H9), 1.34 (m, 4H, H7/H8), 1.70 (m, 2H, H6), 4.26 (t, J(^{1}H,^{1}H) = 6.8 Hz, 2H, H5), 6.36 (d, J(^{1}H,^{1}H) = 12.6 Hz, 1H, H3), 6.42 (d, J(^{1}H,^{1}H) = 12.6 Hz, 1H, H2), 10.29 (s(b), 1H, H1) ppm. ^{13}C NMR ($CDCl_3$, 125.81 MHz): δ = 13.98 (C9), 22.31 (C8), 27.95 (C7), 27.99 (C6), 67.24 (C5), 129.82 (C3), 135.68 (C2), 165.33 (C4), 167.75 (C1) ppm. HR-MS: m/z = 209.0783 g mol^{-1} *vs.* calc. 209.0784 g mol^{-1} [M + Na$^+$].

Synthesis of complex 3a. 1 (400 mg, 1.1 mmol) was suspended in 20 mL of MilliQ water. Ag_2CO_3 (290 mg, 1.1 mmol) and maleic acid (122 mg, 1.1 mmol) were added. The suspension was stirred in the dark at 60 °C for 24 h. The reaction mixture was filtered and the filtrate was allowed to slowly cool down to room temperature. After one night at 4 °C, the precipitate, off white crystals were collected *via* filtration, washed with ice cold water, EtOH and Et_2O. Recrystallization from boiling water and treatment with activated charcoal gave colorless, X-ray quality crystals, which were dried *in vacuo*. Yield 95 mg (20%). A small amount of the crystals was dissolved in hot MilliQ water and lyophilized to improve solubility for the determination of cytotoxicity. ^{1}H NMR (DMF-d_7, 500.32 MHz): δ = 1.16 (m, 4H, H4/H5 ax, isomer A/B), 1.41 (m, 3H, H3/H6 ax, isomer A/B), 1.58 (m, 5H, H4/H5 eq. + H3/H6 ax, isomer A/B), 2.05 (m, 3H, H3/H6 eq., isomer A/B), 2.17 (m, 1H, H3/H6 eq., isomer A/B), 2.35 (m, 4H, H1/H2, isomer A/B), 3.23 (d, J(^{1}H,^{1}H) = 6.7 Hz, 1H, H11, isomer B), 3.29 (s(b), 2H, H14, isomer A/B), 3.35 (d, J(^{1}H,^{1}H) = 6.7 Hz, 1H, H11, isomer A), 3.78 (d, J(^{1}H,^{1}H) = 6.8 Hz, 1H, H10, isomer B), 3.80 (d, J(^{1}H,^{1}H) = 6.8 Hz, 1H, H10, isomer A), 4.20 (t, J(^{1}H,^{1}H) = 10.5 Hz, 1H, H7 ax, isomer A), 4.38 (t, J(^{1}H,^{1}H) = 10.5 Hz, 1H, H7 ax, isomer B), 4.55 (t, J(^{1}H,^{1}H) = 10.4 Hz, 1H, H8 ax, isomer A), 4.82 (m, 1H, H8 eq., isomer B), 5.08 (t, J(^{1}H,^{1}H) = 11.1 Hz, 1H, H8 ax, isomer B), 5.12 (m, 1H, H7 eq., isomer B), 5.21 (m, 1H, H7 eq., isomer A), 5.63 (m, 1H, H8 eq., isomer A), 10.61 (s(b), 1H, H13, isomer A/B) ppm. ^{13}C NMR (DMF-d_7, 125.81 MHz): δ = 19.24 (C11, isomer A), 19.38 (C11, isomer B), 24.54 (C4/C5, isomer A/B), 24.58 (C4/C5, isomer A/B), 24.90 (C4/C5, isomer A/B), 25.01 (C4/C5, isomer A/B), 32.48 (C3/C6, isomer A/B), 32.65 (C3/C6, isomer A/B), 33.70 (C3/C6, isomer A/B), 33.78 (C3/C6, isomer A/B), 58.31 (C1, isomer A), 59.39 (C1, isomer B), 63.19 (C2, isomer B), 63.73 (C2, isomer A), 71.44 (C10, isomer B), 71.60 (C10, isomer A), 178.54 (C9, isomer B), 178.59 (C9, isomer A), 186.36 (C12, isomer B), 186.51 (C12, isomer A) ppm. ^{15}N NMR (DMF-d_7, 50.70 MHz): δ = −38.7 (N8, isomer A), −38.3 (N8, isomer B), 2.7 (N7, isomer A), 2.9 (N7, isomer B) ppm. ^{195}Pt NMR (DMF-d_7, 107.57 MHz): δ = −1280.2 (b, isomer A), −1282.8 (b, isomer B) ppm. EA: ($C_{10}H_{18}N_2O_5Pt$)(H_2O)$_3$; C 24.25%, H 4.88%, N 5.65%; found: C 23.99%, H 4.91%, N 5.65%. HR-MS: m/z = 464.0758 g mol^{-1} *vs.* calc. 464.0757 g mol^{-1} [M + Na$^+$].

General procedure (2) for the synthesis of complexes 3b–3f. **1** (200 mg, 0.53 mmol) was suspended in 10 mL of MilliQ water. Ag_2CO_3 (145 mg, 0.53 mmol) and the respective maleic acid ester (0.53 mmol) were added. After stirring at 60 °C for 24 h, the suspension was diluted with 10 mL of MilliQ water, warmed to 60 °C and filtered. The filtrate was directly purified

 This journal is © The Royal Society of Chemistry 2023

Open Access Article. Published on 06 October 2023. Downloaded on 5/28/2026 2:09:37 PM. This article is licensed under a Creative Commons Attribution-NonCommercial 3.0 Unported Licence.

via preparative HPLC or freeze-dried for storage and redissolved in a small amount of MilliQ water (20–25 mL) for purification *via* preparative HPLC. Subsequently, the HPLC fractions were diluted to an acetonitrile content below 5% (v/v) and lyophilized.

Synthesis of complex 3b. Complex **3b** was synthesized according to general procedure (**2**) from (*Z*)-4-oxo-4-methoxybut-2-enoic acid (68 mg, 0.53 mmol) and purified with 5% acetonitrile.

Yield: 99 mg (41%). ^{1}H NMR (DMF-d$_7$, 500.32 MHz): δ = 1.15 (m, 4H, H4/H5 ax, isomer A/B), 1.33–1.53 (m, 4H, H3/H6 ax, isomer A/B), 1.57 (m, 4H, H4/H5 eq. + H3/H6 ax, isomer A/B), 2.05 (m, 3H, H3/H6 eq., isomer A/B), 2.15 (m, 1H, H3/H6 eq., isomer A/B), 2.33 (m, 4H, H1/H2, isomer A/B), 3.22 (d, $J(^1H,^1H)$ = 6.9 Hz, 1H, H11, isomer A/B), 3.36 (d, $J(^1H,^1H)$ = 6.9 Hz, 1H, H11, isomer A/B), 3.43 (s, 3H, H15, isomer A/B), 3.47 (s, 2H, H15, isomer A/B), 3.81 (d, $J(^1H,^1H)$ = 7.0 Hz, 1H, H10, isomer A/B), 3.83 (d, $J(^1H,^1H)$ = 7.0 Hz, 1H, H10, isomer A/B), 4.24 (t, $J(^1H,^1H)$ = 10.0 Hz, 1H, H7/8 ax, isomer A/B), 4.38 (t, $J(^1H,^1H)$ = 10.5 Hz, 1H, H7/8 ax, isomer A/B), 4.57 (t, $J(^1H,^1H)$ = 9.7 Hz, 1H, H7/8 ax, isomer A/B), 4.84 (d, $J(^1H,^1H)$ = 9.0 Hz, 1H, H7/8 eq., isomer A/B), 5.09 (t, $J(^1H,^1H)$ = 10.3 Hz, 1H, H7/8 ax, isomer A/B), 5.15 (d, $J(^1H,^1H)$ = 10.3 Hz, 1H, H7/8 eq., isomer A/B), 5.22 (d, $J(^1H,^1H)$ = 8.9 Hz, 1H, H7/8 eq., isomer A/B), 5.69 (d, $J(^1H,^1H)$ = 9.4 Hz, 1H, H7/8 eq., isomer A/B) ppm. ^{13}C NMR (DMF-d$_7$, 125.81 MHz): δ = 19.07 (C11, isomer A/B), 19.19 (C11, isomer A/B), 24.48 (C4/C5, isomer A/B), 24.59 (C4/C5, isomer A/B), 24.84 (C4/C5, isomer A/B), 24.98 (C4/C5, isomer A/B), 32.44 (C3/C6, isomer A/B), 32.53 (C3/C6, isomer A/B), 33.62 (C3/C6, isomer A/B), 33.78 (C3/C6, isomer A/B), 49.21 (C15, isomer A/B), 49.31 (C15, isomer A/B), 58.35 (C1, isomer A/B), 59.44 (C1, isomer A/B), 63.40 (C2, isomer A/B), 63.70 (C2, isomer A/B), 71.23 (C10, isomer A/B), 71.36 (C10, isomer A/B), 176.85 (C9, isomer A/B), 176.89 (C9, isomer A/B), 186.46 (C12, isomer A/B), 186.55 (C12, isomer A/B) ppm. ^{15}N NMR (DMF-d$_7$, 50.70 MHz): δ = −39.4 (N7/8, isomer A/B), 2.6 (N7/8, isomer A/B) ppm. ^{195}Pt NMR (DMF-d$_7$, 107.57 MHz): δ = −1274.5 (b, isomer A/B), −1276.5 (b, isomer A/B) ppm. EA: $(C_{11}H_{20}N_2O_5Pt)(H_2O)_{0.5}$: C 28.80% H 4.57% N 5.96%; found: C 28.45% H 4.56% N 6.03%. HR-MS: m/z = 478.0917 g mol^{-1} *vs.* calc. 478.0913 g mol^{-1} [M + Na$^+$].

Synthesis of complex 3c. Complex **3c** was synthesized according to general procedure (**2**) from (*Z*)-4-oxo-4-ethoxybut-2-enoic acid (76 mg, 0.53 mmol) and purified with 5% acetonitrile.

Yield: 107 mg (43%). ^{1}H NMR (DMF-d$_7$, 500.32 MHz): δ = 1.15 (m, 10H, H4/H5 ax + H16, isomer A/B), 1.34–1.66 (m, 8H, H3/H6 ax + H4/H5 eq., isomer A/B), 2.05 (m, 3H, H3/H6 eq., isomer A/B), 2.16 (m, 1H, H3/H6 eq., isomer A/B), 2.34 (m, 4H, H1/H2, isomer A/B), 3.20 (d, $J(^1H,^1H)$ = 6.9 Hz, 1H, H11, isomer A/B), 3.23 (d, $J(^1H,^1H)$ = 5.5 Hz, 2H, H14, isomer A/B), 3.34 (d, $J(^1H,^1H)$ = 7.0 Hz, 1H, H11, isomer A/B), 3.76–3.87 (m, 3H, H10 + H15, isomer A/B), 3.91–4.05 (m, 3H, H15, isomer A/B), 4.24 (t, $J(^1H,^1H)$ = 10.2 Hz, 1H, H7/H8 ax, isomer A/B), 4.43 (m, 2H, H7/H8 ax(A) + H7/H8 eq./ax(B), isomer A/B), 4.65 (d, $J(^1H,^1H)$ = 9.5 Hz, 1H, H7/H8 eq., isomer A/B), 5.15 (m, 2H, H7/H8 eq./ax + H7/H8 ax, isomer A/B), 5.22 (d, $J(^1H,^1H)$ = 8.9 Hz, 1H, H7/H8 eq., isomer A/B), 5.74 (d, $J(^1H,^1H)$ = 9.5 Hz, 1H, H7/H8 eq., isomer A/B) ppm. ^{13}C NMR (DMF-d$_7$, 125.81 MHz): δ = 14.09 (C16, isomer A/B), 14.15 (C16, isomer A/B), 19.28 (C11, isomer A/B), 19.49 (C11, isomer A/B), 24.51 (C4/C5, isomer A/B), 24.59 (C4/C5, isomer A/B), 24.90 (C4/C5, isomer A/B), 25.02 (C4/C5, isomer A/B), 32.53 (C3/C6, isomer A/B), 32.64 (C3/C6, isomer A/B), 33.67 (C3/C6, isomer A/B), 33.82 (C3/C6, isomer A/B), 57.71 (C15, isomer A/B), 57.75 (C15, isomer A/B), 58.34 (C1, isomer A/B), 59.40 (C1, isomer A/B), 63.45 (C2, isomer A/B), 63.79 (C2, isomer A/B), 71.24 (C10, isomer A/B), 71.41 (C10, isomer A/B), 176.22 (C9, isomer A/B), 176.52 (C9, isomer A/B), 186.47 (C12, isomer A/B), 186.59 (C12, isomer A/B) ppm. ^{15}N NMR (DMF-d$_7$, 50.70 MHz): δ = −39.0 (N7/8, isomer A/B), 2.7 (N7/8, isomer A/B) ppm. ^{195}Pt NMR (DMF-d$_7$, 107.57 MHz): δ = −1277.0 (b, isomer A/B), −1285.2 (b, isomer A/B) ppm. EA: $(C_{12}H_{22}N_2O_5Pt)(H_2O)_{0.5}$: C 30.12% H 4.85% N 5.86%; found: C 30.19% H 4.76% N 5.98%. HR-MS: m/z = 492.1070 g mol^{-1} *vs.* calc. 492.1070 g mol^{-1} [M + Na$^+$].

Synthesis of complex 3d. Complex **3d** was synthesized according to general procedure (**2**) from (*Z*)-4-oxo-4-propoxybut-2-enoic acid (84 mg, 0.53 mmol) and purified with 20% acetonitrile.

Yield: 118 mg (46%). ^{1}H NMR (DMF-d$_7$, 500.32 MHz): δ = 0.88 (t, $J(^1H,^1H)$ = 7.3 Hz, 3H, H17, isomer A/B), 0.91 (t, $J(^1H,^1H)$ = 7.5 Hz, 3H, H17, isomer A/B),1.13 (m, 4H, H4/H5 ax, isomer A/B), 1.31–1.63 (m, 12H, H3/H6 ax + H4/H5 eq. + H16, isomer A/B), 2.05 (m, 4H, H3/H6 eq., isomer A/B), 2.32 (m, 4H, H1/H2, isomer A/B), 3.24 (d, $J(^1H,^1H)$ = 7.00 Hz, 1H, H11, isomer A/B), 3.36 (d, $J(^1H,^1H)$ = 6.76 Hz, 1H, H11, isomer A/B), 3.76 (m, 1H, H10, isomer A/B), 3.85 (H15, isomer A/B, taken from HSQC), 3.91 (H10, isomer A/B, taken from HSQC), 4.19 (m, 1H, H7/H8 ax, isomer A/B), 4.36 (m, 2H, H7/H8 ax + H7/H8, isomer A/B), 4.76 (d, $J(^1H,^1H)$ = 10.0 Hz, 1H, H7/H8 eq., isomer A/B), 5.08 (m, 1H, H7/H8 eq., isomer A/B), 5.14 (m, 2H, H7/H8 ax + H7/H8, isomer A/B), 5.78 (d, $J(^1H,^1H)$ = 10.0 Hz, 1H, H7/H8 eq., isomer A/B) ppm. ^{13}C NMR (DMF-d$_7$, 125.81 MHz): δ = 9.88 (C17, isomer A/B), 9.91 (C17, isomer A/B), 19.32 (C11, isomer A/B), 19.52 (C11, isomer A/B), 21.75 (C16, isomer A/B), 21.80 (C16, isomer A/B), 24.17 (C4/C5, isomer A/B), 24.21 (C4/C5, isomer A/B), 24.53 (C4/C5, isomer A/B), 24.61 (C4/C5, isomer A/B), 32.24 (C3/C6, isomer A/B), 32.34 (C3/C6, isomer A/B), 33.28 (C3/C6, isomer A/B), 33.36 (C3/C6, isomer A/B), 58.17 (C1, isomer A/B), 59.01 (C1, isomer A/B), 63.08 (C2, isomer A/B), 63.31 (C2, isomer A/B), 63.70 (C15, isomer A/B), 63.74 (C15, isomer A/B), 71.08 (C10, isomer A/B), 71.20 (C10, isomer A/B), 176.90 (C9, isomer A/B), 176.94 (C9, isomer A/B), 186.54 (C12, isomer A/B), 186.71 (C12, isomer A/B) ppm. ^{195}Pt NMR (DMF-d$_7$, 107.57 MHz): δ = −1273.4 (b, isomer A/B), −1279.9 (b, isomer A/B) ppm. EA: $(C_{13}H_{24}N_2O_5Pt)(H_2O)_{0.5}$: C 31.71% H 5.12% N 5.69%; found: C 31.77% H 5.01% N 5.96%. HR-MS: m/z = 506.1223 g mol^{-1} *vs.* calc. 506.1227 g mol^{-1} [M + Na$^+$].

Synthesis of complex 3e. Synthesized according to general procedure (**2**) from (*Z*)-4-butoxy-4-oxobut-2-enoic acid (91 mg, 0.53 mmol) and purified with 15% acetonitrile.

Open Access Article. Published on 06 October 2023. Downloaded on 5/28/2026 2:09:37 PM. This article is licensed under a Creative Commons Attribution-NonCommercial 3.0 Unported Licence.

Yield: 159 mg (61%). ^{1}H NMR (DMF-d_7, 500.32 MHz): δ = 0.89 (t, $J(^{1}H,^{1}H)$ = 7.3 Hz, 3H, H18, isomer A/B), 0.90 (t, $J(^{1}H,^{1}H)$ = 7.3 Hz, 3H, H18, isomer A/B), 1.15 (m, 4H, H4/H5 ax, isomer A/B), 1.31–1.68 (m, 16H, H4/H5 eq. + H3/H6 ax + H16 + H17, isomer A/B), 2.0–2.17 (m, 4H, H3/H6 eq., isomer A/B), 2.34 (m, 4H, H1/H2, isomer A/B), 3.21 (d, $J(^{1}H,^{1}H)$ = 6.8 Hz, 2H, H11, isomer A/B), 3.24 (m, 2H, H14, isomer A/B), 3.34 (d, $J(^{1}H,^{1}H)$ = 6.9 Hz, 1H, H11, isomer A/B), 3.76–3.85 (m, 3H, H10 + H15, isomer A/B), 3.87–4.03 (m, 3H, H15, isomer A/B), 4.23 (t, $J(^{1}H,^{1}H)$ = 10.3 Hz, 1H, H7/H8 ax, isomer A/B), 4.37 (t, $J(^{1}H,^{1}H)$ = 10.5 Hz, 1H, H7/H8 ax, isomer A/B), 4.44 (t, $J(^{1}H,^{1}H)$ = 10.5 Hz, 1H, H7/H8 ax, isomer A/B), 4.62 (d, $J(^{1}H,^{1}H)$ = 9.2 Hz, 1H, H7/H8 eq., isomer A/B), 5.15 (m, 2H, H7/H8 ax + H7/H8 eq., isomer A/B), 5.23 (m, 1H, H7/H8 eq., isomer A/B), 5.76 (d, $J(^{1}H,^{1}H)$ = 9.1 Hz, 1H, H7/H8 eq., isomer A/B) ppm. ^{13}C NMR (DMF-d_7, 125.81 MHz): δ = 13.36 (C18, isomer A/B), 13.39 (C18, isomer A/B), 19.05 (C17, isomer A/B), 19.08 (C17, isomer A/B), 19.35 (C11, isomer A/B), 19.48 (C11, isomer A/B), 24.47 (C4/C5, isomer A/B), 24.54 (C4/C5, isomer A/B), 24.84 (C4/C5, isomer A/B), 24.95 (C4/C5, isomer A/B), 30.97 (C16, isomer A/B), 31.03 (C16, isomer A/B), 32.53 (C3/C6, isomer A/B), 32.62 (C3/C6, isomer A/B), 33.61 (C3/C6, isomer A/B), 33.73 (C3/C6, isomer A/B), 58.38 (C1, isomer A/B), 59.25 (C1, isomer A/B), 61.72 (C15, isomer A/B), 61.80 (C15, isomer A/B), 63.47 (C2, isomer A/B), 63.66 (C2, isomer A/B), 71.23 (C10, isomer A/B), 71.37 (C10, isomer A/B), 176.47 (C9, isomer A/B), 176.66 (C9, isomer A/B), 186.49 (C12, isomer A/B), 186.67 (C12, isomer A/B) ppm. ^{15}N NMR (DMF-d_7, 50.70 MHz): δ = −39.12 (N7/8, isomer A/B), −38.01 (N7/8, isomer A/B), 2.4 (N7/8, isomer A/B) ppm. ^{195}Pt NMR (DMF-d_7, 107.57 MHz): δ = −1276.3 (b, isomer A/B), −1284.6 (b, isomer A/B) ppm. EA: $(C_{14}H_{26}N_2O_5Pt)(H_2O)$: C 31.62% H 5.48% N 5.44%; found: C 32.70% H 5.38% N 5.38%. HR-MS: m/z = 520.1384 g mol^{-1} *vs.* calc. 520.1383 g mol^{-1} [M + Na^{+}].

Synthesis of complex 3f. Synthesized according to general procedure (**2**) from (*Z*)-4-oxo-4-(pentyloxy)but-2-enoic acid (99 mg, 0.53 mmol) and purified with 21% acetonitrile.

Yield: 117 mg (43%). ^{1}H NMR (DMF-d_7, 500.32 MHz): δ = 0.89 (t, $J(^{1}H,^{1}H)$ = 7.1 Hz, 3H, H19, isomer A/B), 0.90 (t, $J(^{1}H,^{1}H)$ = 6.9 Hz, 3H, H19, isomer A/B), 1.08–1.24 (m, 4H, H4/H5 ax, isomer A/B), 1.26–1.65 (m, 20H, H4/H5 eq. + H3/H6 ax + H16 + H17 + H18, isomer A/B), 2.0–2.17 (m, 4H, H3/H6 eq., isomer A/B), 2.34 (m, 4H, H1/H2, isomer A/B), 3.22 (d, $J(^{1}H,^{1}H)$ = 6.8 Hz, 1H, H11, isomer A/B), 3.24 (m, 1H, H14, isomer A/B), 3.35 (d, $J(^{1}H,^{1}H)$ = 7.0 Hz, 1H, H11, isomer A/B), 3.75–3.85 (m, 3H, H10 + H15, isomer A/B), 3.86–4.03 (m, 3H, H15, isomer A/B), 4.24 (t, $J(^{1}H,^{1}H)$ = 10.22 Hz, 1H, H7/H8 ax, isomer A/B), 4.36 (t, $J(^{1}H,^{1}H)$ = 10.4 Hz, 1H, H7/H8 ax, isomer A/B), 4.45 (t, $J(^{1}H,^{1}H)$ = 10.4 Hz, 1H, H7/H8 ax, isomer A/B), 4.61 (d, $J(^{1}H,^{1}H)$ = 9.5 Hz, 1H, H7/H8 eq., isomer A/B), 5.16 (m, 2H, H7/H8 eq. + H7/H8 ax, isomer A/B), 5.23 (m, 1H, H7/H8 eq., isomer A/B), 5.77 (d, $J(^{1}H,^{1}H)$ = 9.5 Hz, 1H, H7/H8 eq., isomer A/B) ppm. ^{13}C NMR (DMF-d_7, 125.81 MHz): δ = 13.563 (C19, isomer A/B), 13.572 (C19, isomer A/B), 19.32 (C11, isomer A/B), 19.46 (C11, isomer A/B), 22.243 (C18, isomer A/B), 22.255 (C18, isomer A/B), 24.48 (C4/C5, isomer A/B), 24.55 (C4/C5, isomer A/B), 24.85 (C4/C5, isomer A/B), 24.96 (C4/C5, isomer A/B), 28.10 (C17, isomer A/B), 28.14 (C17, isomer A/B), 28.56 (C16, isomer A/B), 28.64 (C16, isomer A/B), 32.56 (C3/C6, isomer A/B), 32.64 (C3/C6, isomer A/B), 33.68 (C3/C6, isomer A/B), 33.76 (C3/C6, isomer A/B), 58.39 (C1, isomer A/B), 59.24 (C1, isomer A/B), 62.05 (C15, isomer A/B), 62.09 (C15, isomer A/B), 63.49 (C2, isomer A/B), 63.67 (C2, isomer A/B), 71.23 (C10, isomer A/B), 71.37 (C10, isomer A/B), 176.44 (C9, isomer A/B), 176.65 (C9, isomer A/B), 186.47 (C12, isomer A/B), 186.66 (C12, isomer A/B) ppm. ^{15}N NMR (DMF-d_7, 50.70 MHz): δ = −39.3 (N7/8, isomer A/B), −38.3 (N7/8, isomer A/B), 2.5 (N7/8, isomer A/B) ppm. ^{195}Pt NMR (DMF-d_7, 107.57 MHz): δ = −1276.2 (b, isomer A/B), −1285.0 (b, isomer A/B) ppm. EA: $(C_{15}H_{28}N_2O_5Pt)(H_2O)$: C 34.02% H 5.71% N 5.29%; found: C 33.89% H 5.63% N 5.29%. HR-MS: m/z = 534.1547 g mol^{-1} *vs.* calc. 534.1540 g mol^{-1} [M + Na^{+}].

Author contributions

Conceptualization, T. M. and M. S. G.; data curation, T. M., N. G., M. H., K. C., and S. M.; formal analysis, T. M., M. H., K. C., and S. M.; funding acquisition, M. A. J., M. S. G., and B. K. K.; investigation, T. M., J. W., N. G., M. H., K. C., and S. M.; methodology, T. M., M. A. J., and M. S. G.; project administration, T. M., M. A. J., M. S. G., and B. K. K.; resources, M. A. J., M. S. G., and B. K. K.; supervision, M. A. J., M. S. G., and B. K. K.; validation, T. M., J. W., N. G., M. H., K. C., and S. M.; visualization, T. M., N. G., M. H., and K. C.; writing – original draft, T. M., M. A. J., and M. S. G.; and writing – review & editing, T. M., J. W., N. G., M. H., K. C., S. M., M. A. J., M. S. G., and B. K. K.

Conflicts of interest

The authors declare that they have no known competing financial interests or personal relationships that could have appeared to influence the work reported in this paper.

Acknowledgements

The authors gratefully acknowledge the support from the University of Vienna. The authors thank the Centre for X-Ray Structure Analysis (University of Vienna) for the determination of the crystal structure. Further, the authors want to thank Martijn Dijkstra for providing oxaliplatin.

References

1 B. Rosenberg, L. Van Camp and T. Krigas, *Nature*, 1965, **205**, 698–699.
2 B. Rosenberg, L. Vancamp, J. E. Trosko and V. H. Mansour, *Nature*, 1969, **222**, 385–386.

 This journal is © The Royal Society of Chemistry 2023

Open Access Article. Published on 06 October 2023. Downloaded on 5/28/2026 2:09:37 PM. This article is licensed under a Creative Commons Attribution-NonCommercial 3.0 Unported Licence.

3 B. Rosenberg and L. VanCamp, *Cancer Res.*, 1970, **30**, 1799–1802.
4 B. Rosenberg, E. Renshaw, L. Vancamp, J. Hartwick and J. Drobnik, *J. Bacteriol.*, 1967, **93**, 716–721.
5 N. J. Wheate, S. Walker, G. E. Craig and R. Oun, *Dalton Trans.*, 2010, **39**, 8113–8127.
6 R. Oun, Y. E. Moussa and N. J. Wheate, *Dalton Trans.*, 2018, **47**, 6645–6653.
7 H. Sung, J. Ferlay, R. L. Siegel, M. Laversanne, I. Soerjomataram, A. Jemal and F. Bray, *CA Cancer J. Clin.*, 2021, **71**, 209–249.
8 P. Forgacs, *Fr. Pat.*, 2558469A1, 1985.
9 L. S. Hollis, S. L. Doran, A. R. Amundsen, E. W. Stern, K. J. Ahmed and S. J. Lippard, in *Inorganic Syntheses*, ed. A. P. Ginsberg, 1990, pp. 283–286.
10 M. A. Mora, A. Raya and M. A. Mora-Ramirez, *Int. J. Quantum Chem.*, 2002, **90**, 882–887.
11 H. Yuge and T. K. Miyamoto, *Acta Crystallogr., Sect. C: Cryst. Struct. Commun.*, 1996, **52**, 3002–3005.
12 H. Yuge and T. K. Miyamoto, *Chem. Lett.*, 1996, **25**, 375–376.
13 Z. X. Huang, Z. Qiu, M. Q. Cheng and X. J. Li, *Chin. Chem. Lett.*, 1991, **2**, 121–122.
14 M. Hrubisko, E. Balázová, F. Kiss, J. Kovácová and V. Ujházy, *Neoplasma*, 1989, **36**, 651–657.
15 L. S. Hollis and E. W. Stern, *Inorg. Chem.*, 1988, **27**, 2826–2831.
16 L. S. Hollis, E. W. Stern, A. R. Amundsen, A. V. Miller and S. L. Doran, *J. Am. Chem. Soc.*, 1987, **109**, 3596–3602.
17 A. R. Amundsen, L. S. Hollis and E. W. Stern, *EU Pat.*, 0174114A1, 1986.
18 L. S. Hollis, A. R. Amundsen and E. W. Stern, *J. Am. Chem. Soc.*, 1985, **107**, 274–276.
19 M. J. Arendse, G. K. Anderson and N. P. Rath, *Inorg. Chem.*, 1999, **38**, 5864–5869.
20 N. Farrell, J. D. Roberts, M. P. Hacker, N. Farrell, J. D. Roberts and M. P. Hacker, *J. Inorg. Biochem.*, 1991, **42**, 237–246.
21 T. W. Failes, M. D. Hall and T. W. Hambley, *Dalton Trans.*, 2003, 1596–1600.
22 V. Sicilia, L. Arnal, S. Fuertes, A. Martín and M. Baya, *Inorg. Chem.*, 2020, **59**, 12586–12594.
23 L. Arnal, S. Fuertes, A. Martín, M. Baya and V. Sicilia, *Chem. – Eur. J.*, 2018, **24**, 18743–18748.
24 H. Leopold, M. Tenne, A. Tronnier, S. Metz, I. Münster, G. Wagenblast and T. Strassner, *Angew. Chem., Int. Ed.*, 2016, **55**, 15779–15782.
25 G. Dahm, E. Borré, G. Guichard and S. Bellemin-Laponnaz, *Eur. J. Inorg. Chem.*, 2015, **2015**, 1665–1668.
26 T. Mihály, M. Bette, B. Mihály, J. Schmidt, H. Schmidt and D. Steinborn, *J. Organomet. Chem.*, 2013, **739**, 57–62.
27 M. Chtchigrovsky, L. Eloy, H. Jullien, L. Saker, E. Ségal-Bendirdjian, J. Poupon, S. Bombard, T. Cresteil, P. Retailleau and A. Marinetti, *J. Med. Chem.*, 2013, **56**, 2074–2086.
28 E. Chardon, G. Dahm, G. Guichard and S. Bellemin-Laponnaz, *Chem. – Asian J.*, 2013, **8**, 1232–1242.
29 E. Chardon, G. Dahm, G. Guichard and S. Bellemin-Laponnaz, *Organometallics*, 2012, **31**, 7618–7621.
30 G. J. Moxey, C. Jones, A. Stasch, P. C. Junk, G. B. Deacon, W. D. Woodul and P. R. Drago, *Dalton Trans.*, 2009, 2630–2636.
31 Y.-L. Ma, R.-J. Zhou, X.-Y. Zeng, Y.-X. An, S.-S. Qiu and L.-J. Nie, *J. Mol. Struct.*, 2014, **1063**, 226–234.
32 H. P. Varbanov, S. Göschl, P. Heffeter, S. Theiner, A. Roller, F. Jensen, M. A. Jakupec, W. Berger, M. S. Galanski and B. K. Keppler, *J. Med. Chem.*, 2014, **57**, 6751–6764.
33 S. Göschl, E. Schreiber-Brynzak, V. Pichler, K. Cseh, P. Heffeter, U. Jungwirth, M. A. Jakupec, W. Berger and B. K. Keppler, *Metallomics*, 2017, **9**, 309–322.
34 D. Höfer, H. P. Varbanov, A. Legin, M. A. Jakupec, A. Roller, M. Galanski and B. K. Keppler, *J. Inorg. Biochem.*, 2015, **153**, 259–271.
35 T. C. Johnstone, K. Suntharalingam and S. J. Lippard, *Chem. Rev.*, 2016, **116**, 3436–3486.
36 G. R. Fulmer, A. J. M. Miller, N. H. Sherden, H. E. Gottlieb, A. Nudelman, B. M. Stoltz, J. E. Bercaw and K. I. Goldberg, *Organometallics*, 2010, **29**, 2176–2179.
37 G. M. Sheldrick, *Acta Crystallogr., Sect. A: Found. Adv.*, 2015, **71**, 3–8.
38 G. M. Sheldrick, *Acta Crystallogr., Sect. C: Struct. Chem.*, 2015, **71**, 3–8.
39 O. V. Dolomanov, L. J. Bourhis, R. J. Gildea, J. A. K. Howard and H. Puschmann, *J. Appl. Crystallogr.*, 2009, **42**, 339–341.
40 C. B. Hübschle, G. M. Sheldrick and B. Dittrich, *J. Appl. Crystallogr.*, 2011, **44**, 1281–1284.
41 K. Valkó, *J. Chromatogr. A*, 2004, **1037**, 299–310.
42 F. Neese, *Wiley Interdiscip. Rev.: Comput. Mol. Sci.*, 2022, **12**, e1606.
43 F. Weigend and R. Ahlrichs, *Phys. Chem. Chem. Phys.*, 2005, **7**, 3297–3305.
44 C. Adamo and V. Barone, *J. Chem. Phys.*, 1999, **110**, 6158–6170.
45 S. Grimme, S. Ehrlich and L. Goerigk, *J. Comput. Chem.*, 2011, **32**, 1456–1465.
46 M. Garcia-Ratés and F. Neese, *J. Comput. Chem.*, 2020, **41**, 922–939.
47 B. Helmich-Paris, B. de Souza, F. Neese and R. Izsák, *J. Chem. Phys.*, 2021, **155**, 104109.
48 F. Weigend, *Phys. Chem. Chem. Phys.*, 2006, **8**, 1057–1065.
49 D. A. Pantazis and F. Neese, *J. Chem. Theory Comput.*, 2011, **7**, 677–684.